JOURNAL OF MATERIALS SCIENCE 35 (2000) 4129–4136

Effect of TiO_2 addition on oxidation behavior of sintered bodies composed of Si_3N_4-Y_2O_3-Al_2O_3-AlN

M. KOBAYASHI, T. MEGURO, K. KOMEYA, T. YOKOYAMA, K. FUNAHASHI
Yokohama National University, 79-5 Tokiwadai, Hodogaya-ku, Yokohama-shi 240-8501, Japan

T. KAMEDA
Heavy Apparatus Engineering Laboratory, Toshiba Co., Ltd., 2-4 Suehirocho, Tsurumi-ku, Yokohama-shi 230-0045, Japan
E-mail: t-meguro@ynu.ac.jp

The effect of TiO_2 content on the oxidation of sintered bodies from the conventional Si_3N_4-Y_2O_3-Al_2O_3-AlN system was investigated. Sintered specimens composed of Si_3N_4, Y_2O_3, Al_2O_3, and AlN, with a ratio of 100 : 5 : 3 : 3 wt% and containing TiO_2 in the range of 0 to 5 wt% to Si_3N_4, were fabricated at 1775 °C for 4 h at 0.5 MPa of N_2. Oxidation at 1200 to 1400 °C for a maximum of 100 h was performed in atmospheres of dry and wet air flows. The relation between weight gain and oxidation time was confirmed to obey the parabolic law. The activation energies decreased with TiO_2 content. In the phases present in the specimens oxidized at 1300 °C for 100 h in dry air, $Y_3Al_5O_{12}$ and TiN, which had existed before oxidation, disappeared. Alpha-cristobalite and $Y_2O_3{\cdot}2TiO_2$ (Y2T) appeared in their place and increased with increasing TiO_2 content. In those oxidized at 1400 °C, α -cristobalite was dominant and very small amounts of $Y_2O_3{\cdot}2SiO_2$ and Y2T were contained. There was a tendency for more α -cristobalite to form in oxidation in wet air than in dry air. Therefore, moisture was confirmed to affect the crystallization of SiO_2 formed during oxidation. Judging from the lower activation energy, the crystallization, and the pores formation, we concluded that the addition of TiO_2 decreases oxidation resistance. © *2000 Kluwer Academic Publishers*

1. Introduction

Silicon nitride (Si_3N_4) ceramics have a variety of superior characteristics, such as high strength, high heat resistance, excellent oxidation and corrosion resistance, low thermal expansion coefficient, and so on. Therefore, Si_3N_4 ceramics have been expected as high-temperature structural materials, especially for engine components and industrial parts [1, 2]. For these applications, high durability at high temperatures in an environment containing oxygen and/or oxidant substances such as water vapor and carbon dioxide is strongly demanded.

Oxidation of Si_3N_4-based ceramics mainly depends on their composition and the microstructure. Since Si_3N_4-based ceramics are mainly composed of Si_3N_4 and/or sialon grains, and grain boundary phase, the oxidation is very complicated. The complexity of oxidation can be found in literature reporting on the corrosion of Si_3N_4-based ceramics, and various activation energies have been reported [3–11]. In most cases, the oxidation of Si_3N_4 leads to the formation of an SiO_2 layer on the surface. The SiO_2 layer is known to retard further oxidation of Si_3N_4 because it plays an important role as a diffusion barrier for oxygen.

Interestingly, the oxidized layer in general Si_3N_4-based ceramics may yield a barrier different from pure SiO_2, corresponding to the composition of the ceramics. This also implies that the oxidation resistance would be dependent on the composition of the additives. In spite of many studies on oxidation, however, the oxidation mechanism has not been yet clarified. The reason seems to be that the composition of each test specimen was not disclosed.

The authors have studied on the oxidation behavior of Si_3N_4-based ceramics developed as wear materials and reported [11] that the activation energy of the oxidation of the specimen containing TiO_2 of 1.5 wt% was extremely low compared to that of a specimen without TiO_2. However, the effect of TiO_2 content on oxidation was ambiguous. In this paper, the effect of TiO_2 addition on the oxidation of sintered bodies of the Si_3N_4-Y_2O_3-Al_2O_3-AlN system was investigated.

2. Experimental

2.1. Raw powders and sintering

In this work, highly pure and very fine grains of α -Si_3N_4 powder (SN-E10) produced by Ube Co., Ltd.

TABLE I Properties of raw powders

Raw powder	[%] O	Impurity [ppm] C	Na	Ca	Fe	BET SSA [m^2/g]	Particle size [μ m]
Si_3N_4	1.19	700	—	<10	<10	11.5	0.67
Y_2O_3	—	—	—	<10	7.3	11.9	0.60
Al_2O_3	—	—	2	2~3	9	10.4	0.21
AlN	0.83	280	—	7	<10	3.4	0.60
TiO_2	—	—	—	—	10	9.4	0.20

was used. The powder was prepared by the imide decomposition method and the α -content is reported to be above 97%. Y_2O_3 (Mitsubishi Chemical Co., Ltd.), Al_2O_3 (Sumitomo Chemical Co., Ltd.), and AlN (Tokuyama Co., Ltd.), were used as sintering aids. TiO_2 (R-11P) supplied by Sakai Chemical Industry was also used as an additive. The properties of the raw powders are shown in Table I.

In this work, sintered specimens containing TiO_2 from 0 to 5 wt% were fabricated to investigate the effect of TiO_2 addition on oxidation. The compositions for fabrication of sintered bodies were prepared as listed in Table II. The parentheses ( ) in Table II means wt%. Hereafter, the names of the specimens without and with TiO_2 are abbreviated as SN00, SN05, SN10, SN15, SN30, and SN50.

The procedure of mixing, molding, and firing was as follows. Raw powders of Si_3N_4, Y_2O_3, Al_2O_3, AlN, and TiO_2 were weighed as shown in Table II and mixed by wet ball milling using a plastic pot with alumina balls for 40 h. Ethanol was used as a dispersant, and an organic binder (Chukyo-yushi SE604) was added. Ethanol was then removed by evaporation. Granules were prepared by passing through a 48 mesh sieve. About 25 g of the granules were uniaxially die-pressed to make a plate with a size of 50 mm × 50 mm and 7 mm thick under 100 MPa, and the plate was dewaxed in a Si_3N_4 powder bed at 600 °C for 4 h under N_2 flow. The plate was then placed on a BN jig set in a graphite crucible in an electric resistance furnace and fired at 1775 °C for 4 h under 0.5 MPa of N_2, applying a heating rate of 20 °C/min.

2.2. Oxidation in dry and wet air

Rectangular bars of test pieces for oxidation, 3 mm × 4 mm × 20 mm in size, were cut from the sintered bodies and machined using a diamond wheel. These specimens were rinsed with acetone and ethanol before the experiment. A specimen was then placed vertically on a SiC-jig and oxidized at 1200, 1300, 1350, and 1400 °C in an alumina reactor tube set in an electric furnace. Oxidation was performed in atmospheres of dry air and wet air flows of 0.5 l/min. Air which was passed through in a silica gel column was used as dry air. The wet air was adjusted to have 2.3 vol% of moisture by bubbling air into a water bath. The oxidation temperature was elevated at a rate of 55 °C/min and the reactor tube was kept at a prescribed oxidation temperature. The specimen was taken out of the reactor tube at regular intervals, weighed after cooling, then put back into the reactor tube to continue the oxidation for a total time of 100 h.

2.3. Evaluation of oxidized specimens

The surfaces of the final resultant specimens after 100 h oxidation were analyzed by X-ray diffraction (XRD) technique. XRD measurement was carried out using a

TABLE III Properties and phases present of the specimens

Specimen	Density (g/cm^3)	Bend strength (MPa)	Phases present
SN00	3.234	490	β -Si_3N_4, Glass phase
SN05	3.180	600	β -Si_3N_4, YAG, TiN
SN10	3.235	600	β -Si_3N_4, YAG, TiN
SN15	3.235	550	β -Si_3N_4, YAG, TiN
SN30	3.238	640	β -Si_3N_4, TiN, YAG
SN50	3.247	530	β -Si_3N_4, TiN, YAG

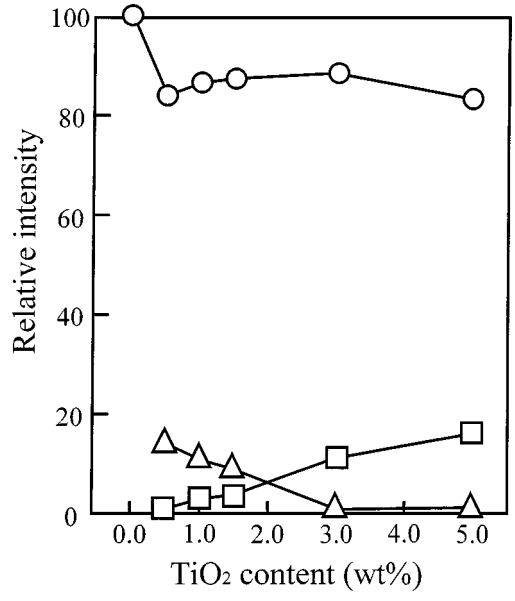

Figure 1 Relation between phases present and TiO_2 content. ○: β-Si_3N_4, △: YAG, □: TiN.

TABLE II Compositions of starting materials. ( ) implies the weight percentages of the additives to be applied to Si_3N_4 100

Specimen	Composition (wt%)				
SN00	Si_3N_4,	Y_2O_3 (5.0),	Al_2O_3 (3.0),	AlN (3.0)	
SN05	Si_3N_4,	Y_2O_3 (5.0),	Al_2O_3 (3.0),	AlN (3.0),	TiO_2 (0.5)
SN10	Si_3N_4,	Y_2O_3 (5.0),	Al_2O_3 (3.0),	AlN (3.0),	TiO_2 (1.0)
SN15	Si_3N_4,	Y_2O_3 (5.0),	Al_2O_3 (3.0),	AlN (3.0),	TiO_2 (1.5)
SN30	Si_3N_4,	Y_2O_3 (5.0),	Al_2O_3 (3.0),	AlN (3.0),	TiO_2 (3.0)
SN50	Si_3N_4,	Y_2O_3 (5.0),	Al_2O_3 (3.0),	AlN (3.0),	TiO_2 (5.0)

Rigaku Denki, RAD-2R diffractometer (Cu K_α radiation). The conditions of the surfaces were also observed by scanning electron microscope (SEM) (Nihondenshi, JSM-T20). Density was measured by Archimedes method with water. Bend strength was evaluated by three points bending test (JIS R1601).

3. Results and discussion

3.1. Specimen before oxidation

Phases present in the specimens containing different amounts of TiO_2 are shown in Fig. 1 and Table III. The values of density and bend strength measured at room temperature are also listed in Table III. The amount of each crystal in the oxidized surfaces were compared using relative intensities of the highest peak. The relative intensity was calculated from the ratio of the maximum peaks in each crystal. In the SN00 specimen, the phase is composed of only β -Si_3N_4, indicating that the grain boundary phase is considered to be forming a glass phase. Containing TiO_2 in the specimens, the phases present are composed of $Y_3Al_5O_{12}$ (YAG) and TiN besides β -Si_3N_4. The YAG phase decreases with increasing TiO_2 content whereas TiN increases. The densities of the specimens are confirmed to be over 98% of the values calculated from the densities of starting materials except of SN05. This fact implies that TiO_2 promotes the densification as a result. It is thought that TiO_2 reacts with Si_3N_4 and/or AlN to produce TiN, SiO_2 and/or Al_2O_3, and the oxides subsequently from a glass phase and YAG. Thus the effect of TiO_2 addition on densification is considered to be based on liquid phase sintering.

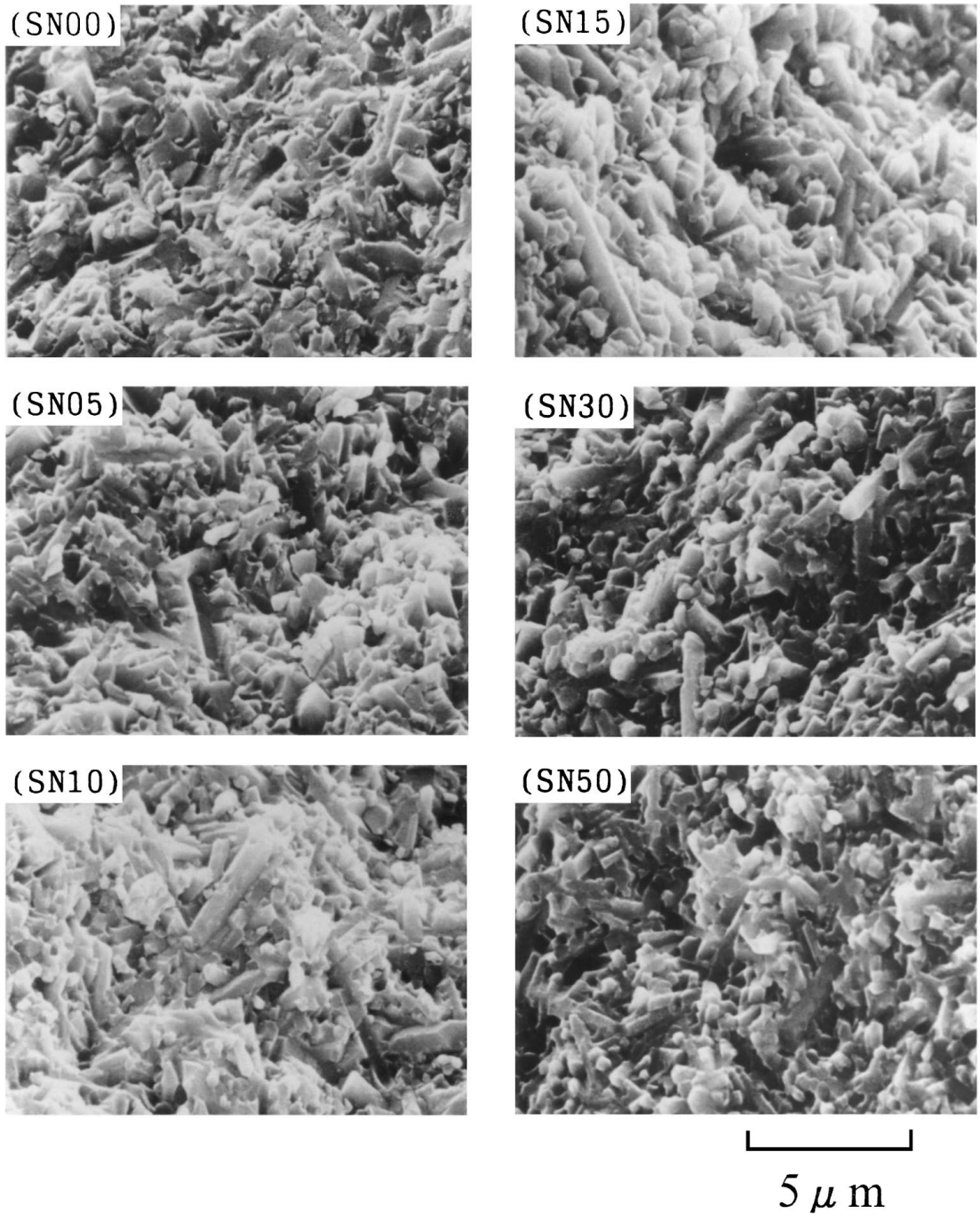

Figure 2 SEM photographs of fractured surfaces of the specimens fabricated with various amount of TiO_2.

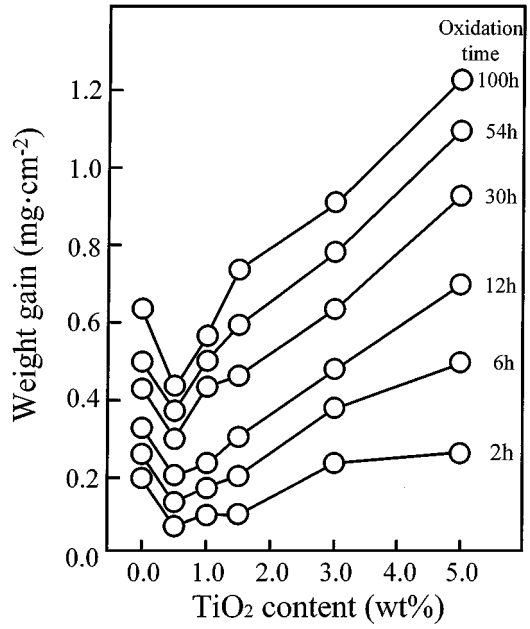

Figure 3 Weight gain in the specimens oxidized at 1300 °C in dry air as a function of TiO_2 content.

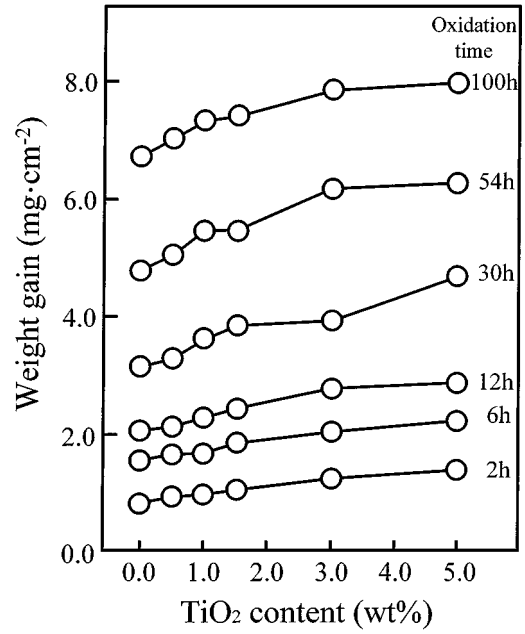

Figure 4 Weight gain in the specimens oxidized at 1400 °C in dry air as a function of TiO_2 content.

SEM photographs of the fractured surfaces of specimens are shown in Fig. 2. Some pores are observed in the specimen SN00 without TiO_2, supporting that the densification is insufficient. The SEM photographs show that the sintered bodies are composed of elongated grain and grain boundary phase and, that the morphology is almost the same in all specimens. However, the elongation is seen to be somewhat remarkable in SN10 and SN15 specimens.

The bend strength of SN00 specimen is relatively low because of the poor sinterability. The other specimens with TiO_2 have almost the same strength as shown in Table III, although there exists more or less scattering of values.

3.2. Oxidation behavior in dry air

Fig. 3 indicates the relationship between weight gain during oxidation at 1300 °C in dry air and TiO_2 content. The weight gains increase with increasing TiO_2 content and reaction time. The increasing tendency of the weight gains in the specimens having more than 1 wt% TiO_2 is particularly remarkable. The weight gain of the SN00 specimen is somewhat larger than that of the SN05 specimen. This is attributed to the microstructure of the SN00 specimen, including pores which permit the diffusion of oxygen toward the inside of the specimen. Excluding this fact, we can conclude that the addition of TiO_2 lowers oxidation resistance.

The results of oxidation at 1400 °C are shown in Fig. 4. The weight gain tends to increase with increasing TiO_2 content as well as in the results at 1300 °C. However, the dependency of TiO_2 content on weight gain is very low compared to the results at 1300 °C. Fig. 4 shows that the extent of oxidation in the specimens without TiO_2 and with low TiO_2 content is considerably large. This means that the mechanism by which the oxidation proceeds differs between 1300 and 1400 °C. This will be discussed again in the following section.

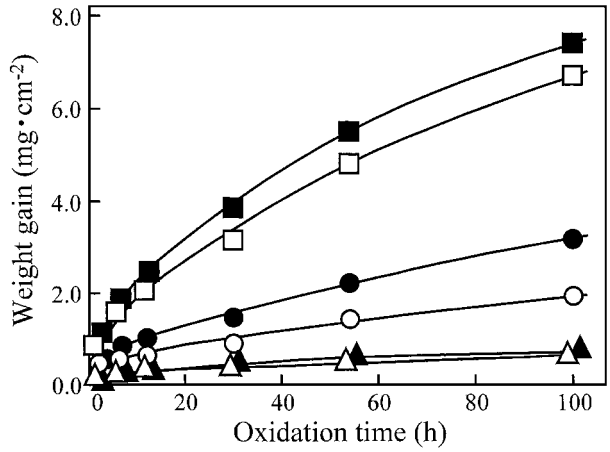

Figure 5 Oxidation time dependence on weight gain of SN00 and SN15 specimens oxidized at various temperatures in dry air. SN00 △: 1300 °C, ○: 1350 °C, □: 1400 °C, SN15 ▲: 1300 °C, ●: 1350 °C, ■: 1400 °C.

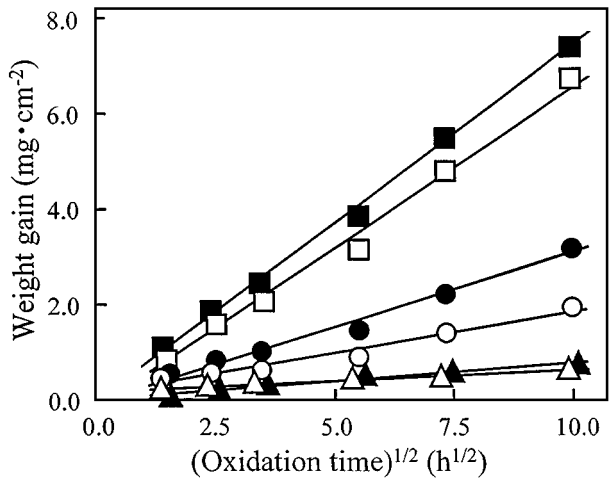

Figure 6 Plots of the weight gain and square root of oxidation time, based on the results of Fig. 5. SN00 △: 1300 °C, ○: 1350 °C, □: 1400 °C, SN15 ▲: 1300 °C, ●: 1350 °C, ■: 1400 °C.

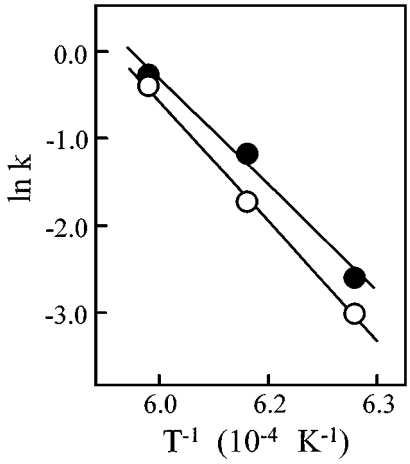

Figure 7 Arrhenius plots of rate constant calculated by adopting the results of Fig. 6 to the parabolic law. ○: SN00, ●: SN15.

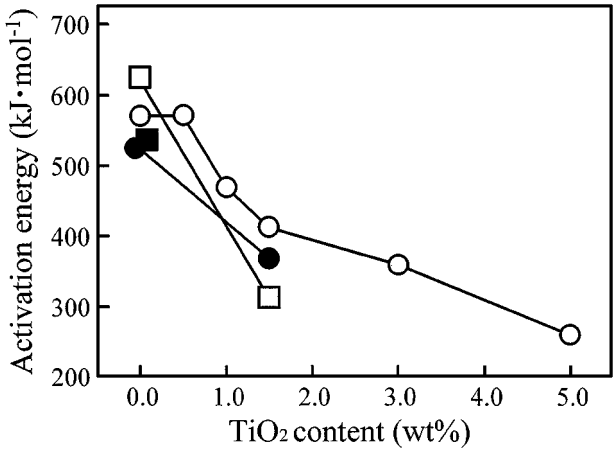

Figure 8 Activation energies on oxidation of the specimens in air as a function of TiO_2 content. ○: in dry air, ●: in wet air, □ and ■: previous work (ref. 11).

The time dependence on weight gain is illustrated in Fig. 5. The data on SN00 and SN15 are selected as typical results. The relationship between weight gain and oxidation time becomes parabolic and a similar tendency was confirmed in other specimens. The plots of the weight gain and square root of oxidation time, based on the results in Fig. 5, are shown in Fig. 6. A good linearity can be observed in all specimens, indicating that the reaction is limited by the diffusion of oxygen according to parabolic law. Arrhenius plots of rate constants obtained from the linear relation of Fig. 6 are shown in Fig. 7. The other data were confirmed to be similarly expressed by a linear relation. The activation energies calculated from each straight line as a function of TiO_2 content are shown in Fig. 8. The data in the figure include the results reported in a previous paper [11]. Almost the same activation energies as reported before are obtained. It is clear that the activation energies of the specimens having more than 1 wt% TiO_2 decrease with increasing TiO_2 content. Generally, a change in the activation energy means a difference in the mechanism of the reaction. In this case, the change in the activation energy seems to be due to the phenomenon that the TiO_2-related compound or composition of the

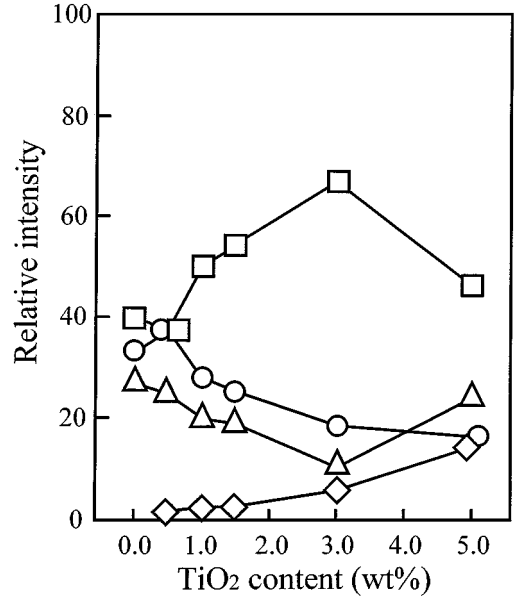

Figure 9 Changes of phases present in the surface layer of the specimens after oxidation at 1300 °C for 100 h in dry air as a function of TiO_2. ○: β -Si_3N_4, □: α -cristobalite, △: $Y_2O_3{\cdot}2SiO_2$, ◇: $Y_2O_3{\cdot}2TiO_2$.

grain boundary phase formed during oxidation is different when the TiO_2 content changes.

3.3. Change of phases present during oxidation

In general, oxidation of Si_3N_4 and sialon yields SiO_2 and α -cristobalite [11]. Si_3N_4-based materials containing Y_2O_3 as a sintering aid form a compound of $Y_2O_3{\cdot}2SiO_2$ (Y2S) [11]. In this study, the results of XRD analysis showed that the phases present were different at each oxidation temperature. Fig. 9 illustrates the changes of the phases present in the surface layer of the specimens after oxidation at 1300 °C for 100 h. The compounds of YAG and TiN existing before oxidation

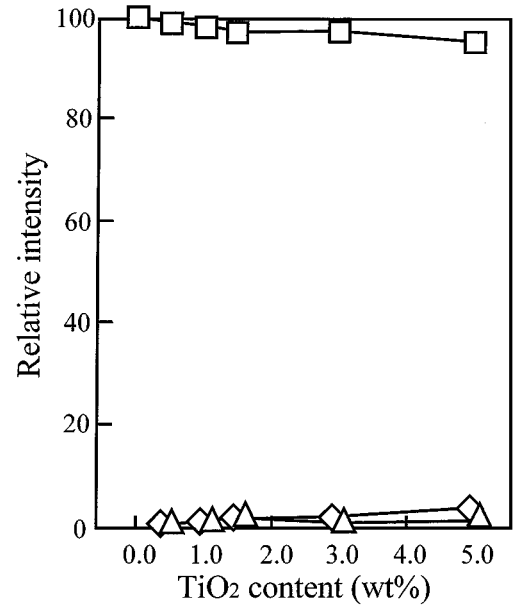

Figure 10 Changes of phases present in the surface layer of the specimens after oxidation at 1400 °C for 100 h in dry air as a function of TiO_2. □: α -cristobalite, △: $Y_2O_3{\cdot}2SiO_2$, ◇: $Y_2O_3{\cdot}2TiO_2$.

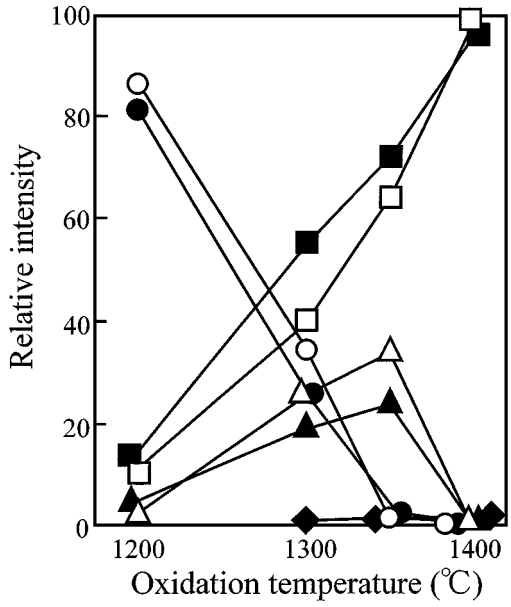

Figure 11 Changes of phases present of the specimens after oxidation at various temperatures for 100 h in dry air. SN00 ○: β -Si_3N_4, □: α -cristobalite, △: $Y_2O_3{\cdot}2SiO_2$, SN15 ●: β -Si_3N_4, ■: α -cristobalite, ▲: $Y_2O_3{\cdot}2SiO_2$, ♦: $Y_2O_3{\cdot}2TiO_2$.

disappear, and α -cristobalite and $Y_2O_3{\cdot}2TiO_2$ (Y2T) increase with increasing TiO_2 content. The formation of Y2T is particularly remarkable when the TiO_2 content exceeds 1.5 wt%. The turning point of the activation energy in Fig. 8 can be seen at 1.5 wt% of TiO_2. This might be due to the formation of Y2T. The increase of Y2T with increasing TiO_2 content indicates that Y_2O_3 reacts more easily with TiO_2 than with SiO_2.

The XRD analysis for the specimens oxidized at 1400 °C reveals that the phases present were composed of α -cristobalite and small amounts of Y2S and Y2T, as shown in Fig. 10. This difference from the result at 1300 °C is considered to be because the surface was covered with a large amount of produced α -cristobalite. Therefore, XRD peaks based on compounds other than α -cristobalite seem to have been very small. The changes of phases present in the surface portions of the SN00 and SN15 specimens oxidized at 1200 to 1400 °C for 100 h are compared in Fig. 11. Beta-Si_3N_4 steeply decreases with increasing temperature, and almost disappears at 1350 °C. It is noteworthy that more α -cristobalite is formed in SN15 oxidized than in SN00 in 1300 and 1350 °C oxidation. The compound Y2S

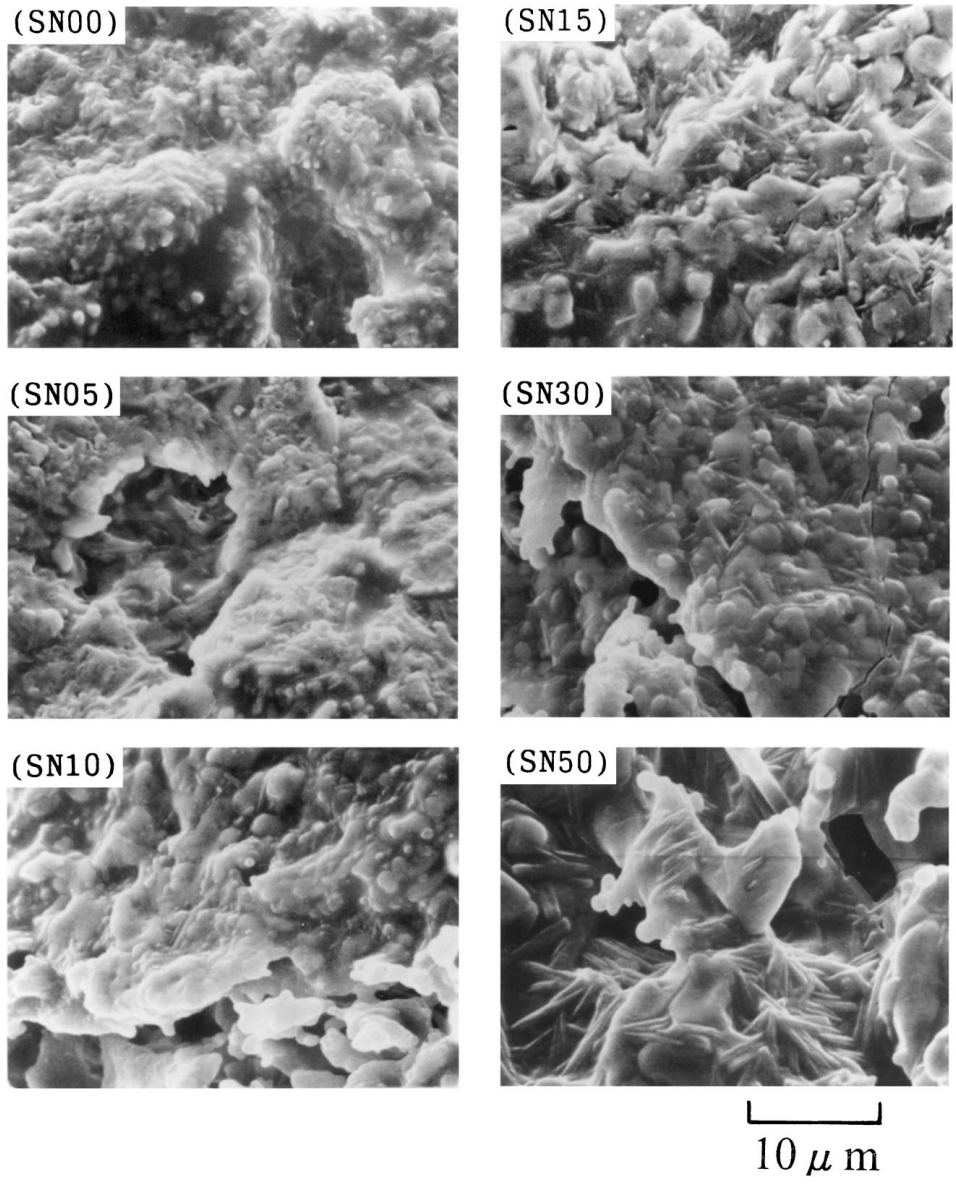

Figure 12 SEM photographs of the specimens oxidized at 1300 °C for 100 h in dry air.

increases with increasing temperature up to 1350 °C and abruptly decreases toward 1400 °C as temperature increases, whereas the yield of α -cristobalite increases with increasing oxidation temperature. The abrupt decrease is considered to be due to the surface coverage by α -cristobalite produced at 1400 °C. It should be noted that the crystallization of the glass phase, or the appearance of α -cristobalite, assists the diffusion of oxygen compared to the glass phase.

3.4. SEM observation

In this work, we used the specimens as-machined, without polishing the surfaces. Therefore the SEM observation of the surfaces of the original specimens offered no information except for their streaked state. The SEM photographs of the surfaces of the specimens after oxidation at 1300 and 1400 °C for 100 h are shown in Figs 12 and 13, respectively. Since the somewhat smoothed surfaces in all specimens after oxidation at 1200 °C for 100 h was confirmed, it was assumed that the surfaces were composed of a thin glass phase containing small sizes of α -cristobalite crystals.

The surfaces of all specimens oxidized at 1300 °C are seen to be covered with roundish crystals and a glass phase. The specimens of SN15 to SN50 also have needle-like crystals. Comparing Fig. 12 with XRD analysis proves that the crystals on the surfaces of the specimens of SN00 to SN30 must be α -cristobalite, and that the needle-like crystal must be Y2T.

Pores are confirmed to exist in the specimens having a large amount of TiO_2, in particular in SN50. The pores are thought to be formed by the evolution of N_2 gas by the reaction of Y2S and TiN with O_2 according to the

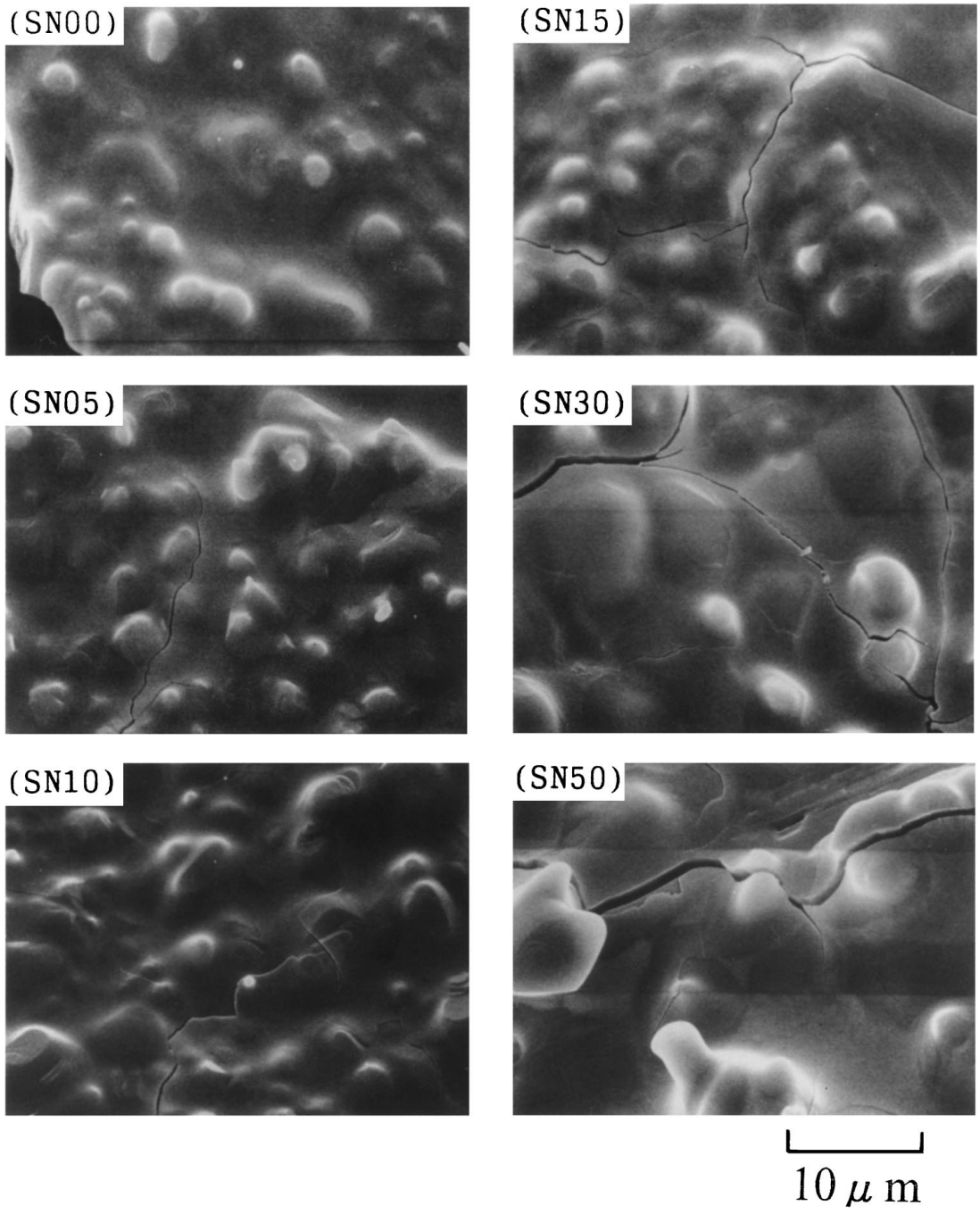

Figure 13 SEM photographs of the specimens oxidized at 1400 °C for 100 h in dry air.

following equation:

$$Y_2Si_2O_7(Y2S) + 2TiN + 2O_2 \rightarrow 2SiO_2 + Y_2Ti_2O_7(Y2T) + N_2.$$

The pores which developed in the specimens during oxidation must promote oxidation in terms of diffusion.

Surfaces oxidized at 1400 °C (Fig. 13) are seen to be covered with a glass phase in all specimens. Crystal grains are also observed in the glass phase, and the size of grains increases with TiO_2 content. Taking XRD results into account, the grains are considered to be mainly α -cristobalite. Some cracks, which seem to arise in the course of cooling, are seen in the specimens of SN15 to SN50.

Judging from the lowering of activation energy, the formation of pores and the enlargement of crystal grains of Y2T, we can conclude that the addition of TiO_2 lowers oxidation resistance.

3.5. Effect of moisture on oxidation

Oxidation of SN00 and SN15 specimens was attempted at 1300 to 1400 °C in wet air. The weight gains in wet air were recognized to increase with the passage of oxidation time. The extent of oxidation at 1300 and 1350 °C was confirmed to somewhat exceed that in dry air. However, the extent of oxidation at 1400 °C in wet air was considerably higher than in dry air. The activation energies calculated from the application of the parabolic law are also plotted in Fig. 8. Lower activation energies are obtained, indicating that moisture promotes the oxidation. The XRD analysis showed that there were no large differences in the phases present in the specimens after oxidation in dry and wet air. However, there was a tendency for α -cristobalite in the specimens oxidized in wet air to be higher than those in dry air. Therefore, moisture might affect the crystallization of SiO_2 formed during oxidation, although the mechanism by which oxidation proceeds in wet air is obscure.

4. Conclusion

This paper has investigated the effect of TiO_2 content on oxidation for sintered bodies of the Si_3N_4-Y_2O_3-Al_2O_3-AlN system. Sintered specimens composed of Si_3N_4, Y_2O_3, Al_2O_3, and AlN, with a ratio of 100 : 5 : 3 : 3 in wt% and containing TiO_2 in the range of 0 to 5 wt% to Si_3N_4, were fabricated by firing at 1775 °C for 4 h at 0.5 MPa of N_2. The names of these specimens were abbreviated according to the TiO_2 content as SN00, SN05, SN10, SN15, SN30, and SN50. Oxidation at 1200 to 1400 °C was performed in atmospheres of dry and wet air flow. The main results and conclusion are as follows:

1. The phase of the SN00 specimen was composed of only β -Si_3N_4, indicating that the grain boundary phase was a glass phase. The phases present in the specimens containing TiO_2 were composed of $Y_3Al_5O_{12}$ (YAG) and TiN besides Si_3N_4.

2. The relation of weight gain and oxidation time in dry air was found to be parabolic, indicating that the reaction is limited by diffusion of oxygen through the oxidized layer. The activation energies decreased with TiO_2 content. A turning point in the relation of activation energy and TiO_2 content was found and was thought to be attributed to the formation of $Y_2O_3 \cdot 2TiO_2$ (Y2T).

3. In oxidation at 1300 °C for 100 h in dry air, YAG and TiN, which had existed before oxidation, changed to α -cristobalite and Y2T increased with increasing TiO_2. The SEM observation in the specimens oxidized at 1300 °C showed that the surfaces were covered with roundish grains and a glass phase, and that the specimens of SN15, SN30, and SN50 also had needle-like crystals. Comparing XRD analysis with SEM observation indicated that the grains and the needle-like crystals were α -cristobalite and Y2T, respectively.

4. In the phases present in the specimens oxidized at 1400 °C for 100 h in dry air, α -cristobalite was dominant and there were very small amounts of Y2S and Y2T. The composition dependence of α -cristobalite formation was not found. The SEM observation of the specimens oxidized at 1400 °C showed that the surfaces of all specimens were covered with a glass phase and grains which seemed to be α -cristobalite.

5. In the specimens of SN00 and SN15 oxidized at 1200 to 1400 °C, α -cristobalite increased with increasing oxidation temperature, and Y2S increased with increasing temperature up to 1350 °C and abruptly decreased as temperature further increased toward 1400 °C.

6. Judging from the lower activation energy, the crystallization of α -cristobalite and Y2T, and the pore formation, we concluded that the addition of TiO_2 lowers oxidation resistance.

7. The XRD analysis for the specimens oxidized in wet air flow showed that the essential phases present were essentially almost the same as those oxidized in dry air flow. However, the amount of α -cristobalite formed in the specimens oxidized in wet air tends to be higher than that in dry air. Therefore, moisture was confirmed to affect the crystallization of SiO_2 formed during oxidation.

References

1. K. KOMEYA and M. MATSUI, "Materials Science and Technology, Vol. 11: Structure and Properties of Ceramics," edited by M. V. Swain (VCH, Germany, 1994) p. 517.
2. H. KAWAMURA, in 6th International Symposium on Ceramic Materials and Components for Engines, Tokyo, 1998, edited by K. Niihara *et al*. p. 5.
3. R. M. HORTON, *J. Am. Ceram. Soc*. **52** (1969) 121.
4. P. GOURSAT, P. LORTHOLARY, D. TENTAND and M. BILLY, in Proceedings of the 7th International Symposium on Reactivity of Solids, Bristol, 1972, p. 315.
5. S. C. SINGHAL, *J. Mater. Sci*. **11** (1976) 500.
6. *Idem., J. Am. Ceram. Soc*. **59** (1976) 81.
7. W. C. TRIPP and H. C. GRAHAM, *ibid*. **59** (1976) 339.
8. D. CUBICCIOTI and K. H. LAU, *ibid*. **61** (1978) 512.
9. G. N. BABINI, A. BELLOSI and P. VINCENZINI, *ibid*. **64** (1981) 578.
10. T. SATO, K. HARYU, T. ENDO and M. SHIMADA, *J. Mater. Sci*. **22** (1987) 2635.
11. K. KOMEYA, Y. HARUNA, T. MEGURO, T. KAMEDA and M. ASAYAMA, *ibid*. **27** (1992) 5727.

Received 23 June 1999
and accepted 19 January 2000